

# Substitution Lability of the Perfluorinated Cp\* Ligand in [Rh(COD)(C<sub>5</sub>(CF<sub>3</sub>)<sub>5</sub>)] Towards Triphenylpnictogens EPh<sub>3</sub> (E = N, P, As, Sb, Bi)

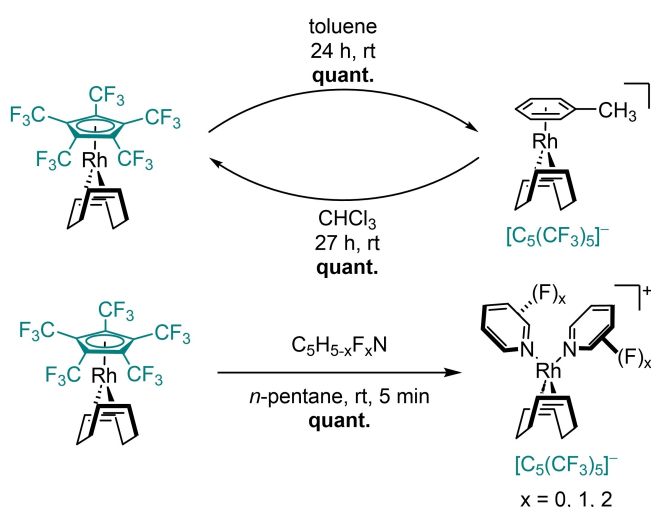
Nico G. Kub,<sup>[a]</sup> Robin Sievers,<sup>[a]</sup> Joshua Parche,<sup>[a]</sup> and Moritz Malischewski\*<sup>[a]</sup>

Triphenylpnictogens EPh<sub>3</sub> (E=N, P, As, Sb, Bi) are able to displace the perfluorinated Cp\* ligand in [Rh(COD)(C<sub>5</sub>(CF<sub>3</sub>)<sub>5</sub>)] (COD=1,5-cyclooctadiene) in up to quantitative yield. The resulting ionic products contain [C<sub>5</sub>(CF<sub>3</sub>)<sub>5</sub>]<sup>−</sup> as uncoordinated counter anion. The cations feature [Rh(COD)]<sup>+</sup> fragments,

coordinated by one (N, Bi), two (P, As) or three (Sb) triphenylpnictogen moieties. Whereas coordination via the pnictogen is observed for P, As and Sb,  $\pi$ -coordination of the aryl rings is observed for N and Bi.

## Introduction

In contrast to ordinary electron rich cyclopentadienyl (Cp) ligands, highly fluorinated Cp ligands display unique chemical properties due to their decreased  $\pi$ -donor abilities. Unfortunately, there are only a few such complexes, as both the fluorinated Cp ligands and their complexes are very difficult to access synthetically.<sup>[1]</sup> Generally, the introduction of highly fluorinated alkyl chains enables the solubility of transition metal complexes in perfluorinated solvents, relevant in the field of biphasic catalysis.<sup>[2]</sup> The insertion of one or multiple electron withdrawing CF<sub>3</sub> substituents into a Cp ligand fundamentally changes the redox behavior of a complex, by increasing its oxidative stability.<sup>[3]</sup> While ordinary Cp ligands usually exhibit strong binding energies and require harsh reductive conditions for their removal,<sup>[4]</sup> fluorinated Cp derivatives usually display lower binding energies<sup>[1]</sup> and should consequently be more substitution labile. In previous works we showed the first coordination of [C<sub>5</sub>(CF<sub>3</sub>)<sub>5</sub>]<sup>−</sup> to give the stable [Rh(COD)(C<sub>5</sub>(CF<sub>3</sub>)<sub>5</sub>)] transition metal complex, which undergoes a unique reversible substitution of [C<sub>5</sub>(CF<sub>3</sub>)<sub>5</sub>]<sup>−</sup> by toluene (Scheme 1, top).<sup>[5]</sup> Our subsequent work further exemplified the displacement of [C<sub>5</sub>(CF<sub>3</sub>)<sub>5</sub>]<sup>−</sup> with several fluorinated pyridines (Scheme 1, bottom).<sup>[6]</sup> The weakly binding character of the [C<sub>5</sub>(CF<sub>3</sub>)<sub>5</sub>]<sup>−</sup> ligand makes [Rh(COD)(C<sub>5</sub>(CF<sub>3</sub>)<sub>5</sub>)] an useful synthetic equivalent of the 12-electron [Rh(COD)]<sup>+</sup> fragment to access various coordination compounds.



**Scheme 1.** Quantitative reversible substitution of [C<sub>5</sub>(CF<sub>3</sub>)<sub>5</sub>]<sup>−</sup> in [Rh(COD)(C<sub>5</sub>(CF<sub>3</sub>)<sub>5</sub>)] through toluene (top) and through fluorinated pyridines (bottom).<sup>[5–6]</sup>

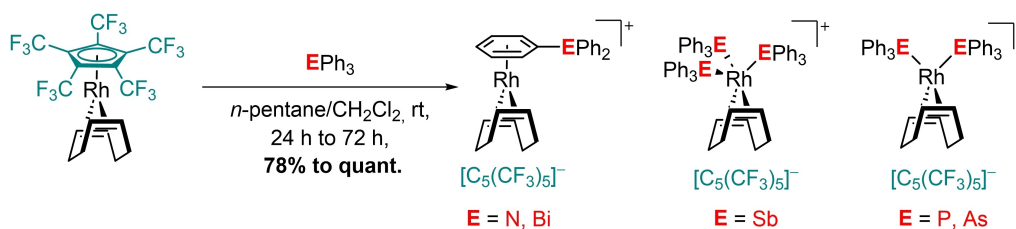
Besides the Cp ligand, the class of phosphine ligands is arguably one of the most prevalent ligand systems in organometallic chemistry. Phosphines find a wide range of applications in catalysis and shaped the last decades of coordination chemistry, with PPh<sub>3</sub> likely being the most prominent phosphine.<sup>[7]</sup>

A database survey in the Cambridge Crystallographic Data Centre (CCDC) revealed more than 30000 transition metal complexes containing at least one PPh<sub>3</sub> ligand. While the arsine analogue AsPh<sub>3</sub> still poses as a good donor ligand, the increasingly diminishing nucleophilicity of the stibine and bismuthine analogues, SbPh<sub>3</sub> and BiPh<sub>3</sub>, restrict their coordination to only a few transition metal compounds.<sup>[7d,8]</sup> Especially for BiPh<sub>3</sub> the number of transition metal complexes is limited to nine complexes due to the combination of weak donor ability and reactive Bi–C bonds, decomposing in the presence of many metals.<sup>[8a,b]</sup> Due to the diminished nucleophilicity of BiPh<sub>3</sub>, coordination can take place either via the central atom or  $\pi$ -coordination of the phenyl groups.<sup>[9]</sup> The general trend of

[a] N. G. Kub, R. Sievers, J. Parche, Dr. M. Malischewski  
Institute of Chemistry and Biochemistry – Inorganic Chemistry  
Freie Universität Berlin  
Fabeckstr. 34/36, 14195 Berlin, Germany  
E-mail: moritz.malischewski@fu-berlin.de

Supporting information for this article is available on the WWW under <https://doi.org/10.1002/chem.202400427>

© 2024 The Authors. Chemistry - A European Journal published by Wiley-VCH GmbH. This is an open access article under the terms of the Creative Commons Attribution License, which permits use, distribution and reproduction in any medium, provided the original work is properly cited.



Scheme 2. Substitution of  $[\text{C}_5(\text{CF}_3)_5]^-$  in  $[\text{Rh}(\text{COD})(\text{C}_5(\text{CF}_3)_5)]$  by  $\text{EPh}_3$  ( $\text{E} = \text{N}, \text{P}, \text{As}, \text{Sb}, \text{and Bi}$ ).

decreasing nucleophilicity of triarylpnictogens as one descends in the periodic table can be described through enlarged  $\sigma$ -donor orbitals and their decreased electron densities, leading to a weakening of the  $\sigma$ -donor ability. Similarly, the ability of  $\pi$ -back bonding acceptance tends to decrease from  $\text{PR}_3$  to  $\text{BiR}_3$ .<sup>[8a,b, 10]</sup> Mentioning  $\text{EPh}_3$  group 15 ligands,  $\text{NPh}_3$  is an anomaly to this trend, due to the delocalized nitrogen lone pair, reflected by its trigonal planar structure.<sup>[11]</sup> To this date, only a single transition metal complex containing  $\text{NPh}_3$  as a ligand is known, in which  $\text{NPh}_3$  coordinates via an  $\eta^6$ -arene bond.<sup>[12]</sup>

The works of Schuman *et al.* and Lappert *et al.* have demonstrated the changes in group 15  $\text{EPh}_3$  ligand donor properties, although both were missing the comparison to  $\text{NPh}_3$ .<sup>[13]</sup> Due to the  $[\text{Fe}(\text{C}_5\text{H}_5)(\text{CO})_2]^+$  and  $[\text{Cr}(\text{CO})_5]$  16-electron fragments being employed in those works, the coordination of the  $\text{EPh}_3$  pnictogens occurs only via the pnictogen, restricting the structural diversity.

In this work we demonstrate the nucleophilicity of group 15  $\text{EPh}_3$  ligands with regards to the displacement of  $[\text{C}_5(\text{CF}_3)_5]^-$ . Since the easily accessible  $[\text{Rh}(\text{COD})]^+$  fragment supports both  $\eta^6$ -arene bound ligands as well as  $\sigma$ -bound ligands, the preferred binding modes for the respective pnictogens can be identified and compared (Scheme 2).

## Results and Discussion

$[\text{NEt}_4][\text{C}_5(\text{CF}_3)_5]$  was synthesized according to the procedure of Chambers *et al.* from hexachlorobuta-1,4-diene.<sup>[14]</sup> The subsequent coordination of  $[\text{C}_5(\text{CF}_3)_5]^-$  to produce  $[\text{Rh}(\text{COD})(\text{C}_5(\text{CF}_3)_5)]$  was performed following the procedure of Malischewski *et al.*<sup>[5]</sup> All substitution reactions utilizing the  $\text{EPh}_3$  ligands, with  $\text{E} = \text{N}, \text{P}, \text{As}, \text{Sb}, \text{and Bi}$ , could either be carried out in *n*-pentane or  $\text{CH}_2\text{Cl}_2$ . When possible, reactions in *n*-pentane were preferred, due to the precipitation of the respective salts, enabling a complete conversion. Quantitative yields were obtained for all substitution reactions, except for  $\text{BiPh}_3$ , with a yield of 78%.

Reactions performed in  $\text{CH}_2\text{Cl}_2$  could be monitored via  $^{19}\text{F}$  NMR spectroscopy, by integrating and comparing the signals of ionic ( $\delta = -50.5$  ppm in  $\text{CH}_2\text{Cl}_2$ ) and coordinated  $[\text{C}_5(\text{CF}_3)_5]^-$  ( $\delta = -51.5$  ppm in  $\text{CH}_2\text{Cl}_2$ ), in analogy to the previous substitution by toluene, acetonitrile, and fluorinated pyridines.<sup>[5-6]</sup> Unreacted  $[\text{Rh}(\text{COD})(\text{C}_5(\text{CF}_3)_5)]$  and other impurities were removed by washing the adducts with *n*-pentane.

### $[\text{Rh}(\text{COD})(\eta^6\text{-NPh}_3)][\text{C}_5(\text{CF}_3)_5]$

After successful displacement of  $[\text{C}_5(\text{CF}_3)_5]^-$ , clearly shown in the  $^{19}\text{F}$  NMR spectrum through a signal shift from coordinated to ionic  $[\text{C}_5(\text{CF}_3)_5]^-$ , the  $^1\text{H}$  NMR spectrum of  $[\text{Rh}(\text{COD})(\eta^6\text{-NPh}_3)][\text{C}_5(\text{CF}_3)_5]$  shows two inequivalent sets of signals for the phenyl substituents of  $\text{NPh}_3$  with an integral ratio of 2:1. This indicates a  $\eta^6$ -arene coordination of one phenyl ring of  $\text{NPh}_3$  to Rh. Single crystals of the respective salt were obtained by vapor diffusion of  $\text{CH}_2\text{Cl}_2$  and *n*-pentane, crystallizing in the triclinic space group  $P\bar{1}$ . The asymmetric unit containing  $[\text{Rh}(\text{COD})(\eta^6\text{-NPh}_3)][\text{C}_5(\text{CF}_3)_5]$  moieties confirms this structural motive (Figure 1).

The solid state structure reveals an average Rh–C bond length of 2.312(6) Å to the arene substituent and 2.146(7) Å to the COD ligand. Since  $[\text{Re}(\eta^6\text{-NPh}_3)_2][\text{PF}_6]$  is the only known complex containing  $\text{NPh}_3$  as a ( $\pi$ -bound) ligand,  $[\text{Rh}(\text{COD})(\eta^6\text{-NPh}_3)][\text{C}_5(\text{CF}_3)_5]$  represents a rare example, further extending the  $\text{NPh}_3$  coordination chemistry.<sup>[12]</sup>

### $[\text{Rh}(\text{COD})(\text{PPh}_3)_2][\text{C}_5(\text{CF}_3)_5]$

The  $^1\text{H}$  NMR spectrum of  $[\text{Rh}(\text{COD})(\text{PPh}_3)_2][\text{C}_5(\text{CF}_3)_5]$  supports a twofold  $\sigma$ -coordination of  $\text{PPh}_3$ , with a substituent ratio of 2:1 for  $\text{PPh}_3$  against COD. Single crystals of  $[\text{Rh}(\text{COD})(\text{PPh}_3)_2][\text{C}_5(\text{CF}_3)_5]$  were obtained by slowly cooling a  $\text{SO}_2$  solution to  $-75^\circ\text{C}$ . The respective salt crystallizes in the triclinic space group  $P\bar{1}$ , with one  $[\text{Rh}(\text{COD})(\text{PPh}_3)_2][\text{C}_5(\text{CF}_3)_5]$  moiety in the asymmetric unit, confirming a twofold coordination of  $\text{PPh}_3$  towards Rh (Figure 2).

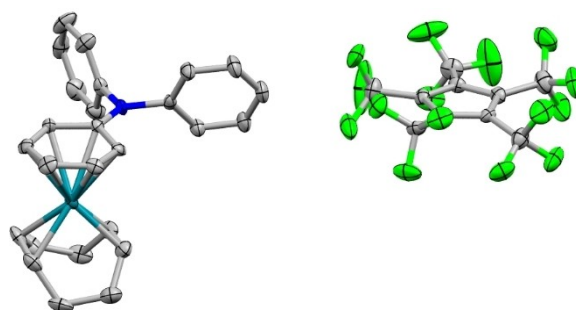
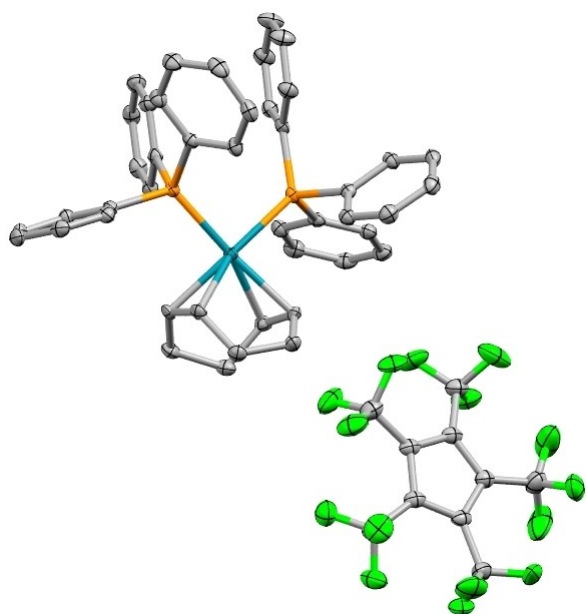


Figure 1. Molecular structure in solid state of  $[\text{Rh}(\text{COD})(\eta^6\text{-NPh}_3)][\text{C}_5(\text{CF}_3)_5]$ . Disorders, hydrogens, and solvent molecules are omitted for clarity. Ellipsoids are depicted with 50% probability level. Color code: grey-carbon; green-fluorine, blue-nitrogen, light-blue-rhodium.



**Figure 2.** Molecular structure in solid state of  $[\text{Rh}(\text{COD})(\text{PPh}_3)_2][\text{C}_5(\text{CF}_3)_5]$ . Hydrogens and solvent molecules are omitted for clarity. Ellipsoids are depicted with 50% probability level. Color code: grey-carbon; green-fluorine, orange-phosphor, light-blue-rhodium.

The solid state structure reveals an averaged Rh–P bond length of 2.3390(7) Å and an averaged Rh–C bond length of 2.2449(26) Å to the COD ligand, similar to the bond lengths of  $[\text{Rh}(\text{COD})(\text{PPh}_3)_2][\text{BF}_4]$  with an averaged Rh–P bond length of 2.3419(11) Å and an averaged Rh–C bond length of 2.2470(40) Å to the COD ligand.<sup>[15]</sup> Since the  $[\text{Rh}(\text{COD})(\text{PPh}_3)_2]^+$  structural motive is of interest due to its catalytical properties regarding the hydroformylation of olefins,<sup>[15]</sup> our new synthetic route should provide an alternative access to such complexes.

#### $[\text{Rh}(\text{COD})(\text{AsPh}_3)_2][\text{C}_5(\text{CF}_3)_5]$

Similarly, to the corresponding adduct of  $\text{PPh}_3$ , the  $^1\text{H}$  NMR spectrum of  $[\text{Rh}(\text{COD})(\text{AsPh}_3)_2][\text{C}_5(\text{CF}_3)_5]$  shows an integral ratio of 2:1 between the  $\text{AsPh}_3$  fragments and COD, indicating a  $\sigma$ -coordination of two  $\text{AsPh}_3$  moieties. For structural confirmation, single crystals of  $[\text{Rh}(\text{COD})(\text{AsPh}_3)_2][\text{C}_5(\text{CF}_3)_5]$  were obtained by slowly cooling a mixture of  $\text{CH}_2\text{Cl}_2$  and *n*-pentane to  $-75^\circ\text{C}$ . The compound crystallizes in the triclinic space group  $P\bar{1}$ . The asymmetric unit contains one  $[\text{Rh}(\text{COD})(\text{AsPh}_3)_2][\text{C}_5(\text{CF}_3)_5]$  fragment, providing the  $\sigma$ -coordination of two  $\text{AsPh}_3$  moieties. The solid state structure reveals an average Rh–As bond length of 2.4459(5) Å and 2.2048(36) Å to the COD ligand. While Rh(I) complexes containing  $\text{AsPh}_3$  as a ligand exist,  $[\text{Rh}(\text{COD})(\text{AsPh}_3)_2][\text{C}_5(\text{CF}_3)_5]$  is the first Rh(I) complex with a twofold  $\text{AsPh}_3$  and onefold COD coordination, making it a unique example of As coordination chemistry.

#### $[\text{Rh}(\text{COD})(\text{SbPh}_3)_3][\text{C}_5(\text{CF}_3)_5]$

The  $^1\text{H}$  NMR spectrum of  $[\text{Rh}(\text{COD})(\text{SbPh}_3)_3][\text{C}_5(\text{CF}_3)_5]$  indicates a threefold coordination of the  $\text{SbPh}_3$  moiety, with a substituent ratio of 3:1 for  $\text{SbPh}_3$  against COD, respectively. Single crystals of the compound were obtained through vapor diffusion using  $\text{CH}_2\text{Cl}_2$  and *n*-pentane. The respective salt crystallized in the monoclinic space group  $P2_1/n$  with one  $[\text{Rh}(\text{COD})(\text{SbPh}_3)_3][\text{C}_5(\text{CF}_3)_5]$  fragment in the asymmetric unit, confirming the threefold coordination of the  $\text{SbPh}_3$  moiety (Figure 3).

Additionally, the solid state structure revealed an averaged Rh–Sb bond length of 2.6321(6) Å and an average Rh–C bond length of 2.2146(30) Å to the COD ligand. A database survey in the Cambridge Crystallographic Database (CCDC) revealed a total of 28 rhodium complexes containing  $\text{SbPh}_3$ . However, none of them contain the  $[\text{Rh}(\text{COD})]^+$  fragment, thus rendering  $[\text{Rh}(\text{COD})(\text{SbPh}_3)_3][\text{C}_5(\text{CF}_3)_5]$  an important extension of  $\text{SbPh}_3$  coordination chemistry.

#### $[\text{Rh}(\text{COD})(\eta^6\text{-BiPh}_3)][\text{C}_5(\text{CF}_3)_5]$

In contrast to the other corresponding adduct complexes of  $\text{NPh}_3$ ,  $\text{PPh}_3$ ,  $\text{AsPh}_3$  and  $\text{SbPh}_3$ ,  $[\text{Rh}(\text{COD})(\eta^6\text{-BiPh}_3)][\text{C}_5(\text{CF}_3)_5]$  could only be synthesized in  $\text{CH}_2\text{Cl}_2$ , as any attempts using *n*-pentane as a solvent lead to unspecific decomposition. During the reaction in  $\text{CH}_2\text{Cl}_2$ , the slow precipitation of a black solid also indicates the decay of  $[\text{Rh}(\text{COD})(\eta^6\text{-BiPh}_3)][\text{C}_5(\text{CF}_3)_5]$ , limiting the reaction time to 24 h with an incomplete conversion. The  $^1\text{H}$  NMR spectrum indicates the coordination of one  $\text{BiPh}_3$  entity with two chemically different signal sets for the phenyl substituents, showing an integral ratio of 2:1 and supporting the structural motive of an  $\eta^6$ -arene bound  $\text{BiPh}_3$  ligand (similar to  $\text{NPh}_3$ ). Single crystals of the corresponding salt were obtained by slowly cooling from a mixture of  $\text{CH}_2\text{Cl}_2$  and *n*-pentane to  $-75^\circ\text{C}$ . The compound crystallized in the triclinic

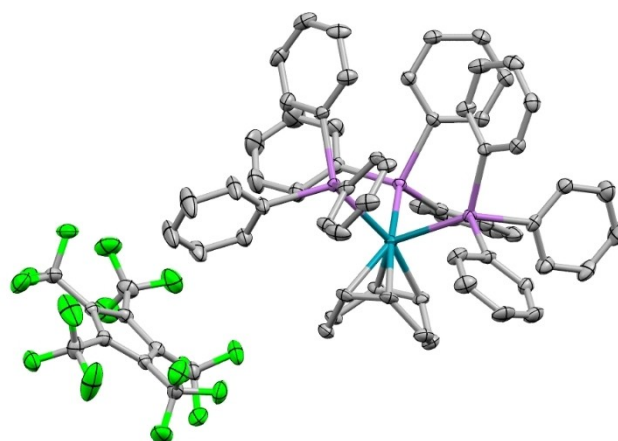


**Figure 3.** Molecular structure in solid state of  $[\text{Rh}(\text{COD})(\text{SbPh}_3)_3][\text{C}_5(\text{CF}_3)_5]$ . Hydrogens are omitted for clarity. Ellipsoids are depicted with 50% probability level. Color code: grey-carbon; green-fluorine, purple-antimony, light-blue-rhodium.

space group  $P\bar{1}$  with one  $[\text{Rh}(\text{COD})(\eta^6\text{-BiPh}_3)][\text{C}_5(\text{CF}_3)_5]$  moiety in the asymmetric unit, reinforcing the onefold coordination of  $\text{BiPh}_3$  via an  $\eta^6$ -bound phenyl substituent (Figure 4). The solid state structure reveals an average Rh–C bond length of 2.3064(48) Å to the arene substituent and 2.1446(46) to the COD ligand. Since the number transition metal complexes containing  $\text{BiPh}_3$  is scarce,  $[\text{Rh}(\text{COD})(\eta^6\text{-BiPh}_3)][\text{C}_5(\text{CF}_3)_5]$  represents a rare example in the Bi coordination chemistry.

## Conclusions

In conclusion, the weak bonding interactions of the  $[\text{C}_5(\text{CF}_3)_5]^-$  ligand towards the  $[\text{Rh}(\text{COD})]^+$  fragment enabled its substitution and the structural characterization of the first complete series of  $\text{EPh}_3$  ( $\text{E} = \text{N}, \text{P}, \text{As}, \text{Sb}, \text{Bi}$ ) coordination chemistry. Hereby, the versatility of the 12-electron fragment  $[\text{Rh}(\text{COD})]^+$  allows for a full demonstration of the varying nucleophilicity of the  $\text{EPh}_3$  ligands depending on the central atom, affecting the coordination mode of the respective ligand.  $\text{PPh}_3$  and  $\text{AsPh}_3$  are strong  $\sigma$ -donors and therefore prefer a coordination via the pnictogen, resulting in a twofold coordination of the respective ligands. While  $\text{SbPh}_3$  is still  $\sigma$ -bound over the pnictogen, the diminished nucleophilicity and its larger size lead to an elongation of the Rh–Sb  $\sigma$ -bond, allowing for a threefold coordination of  $\text{SbPh}_3$ . In contrast,  $\text{NPh}_3$  and  $\text{BiPh}_3$  exhibit reduced nucleophilicities at the central atom and therefore prefer coordination via  $\eta^6$ -arene bonding. Furthermore, newly synthesized  $[\text{Rh}(\text{COD})(\eta^6\text{-$

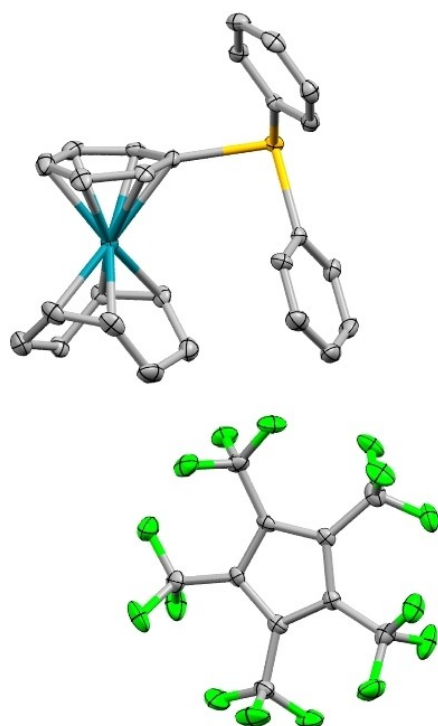


**Figure 4.** Molecular structure in solid state of  $[\text{Rh}(\text{COD})(\eta^6\text{-BiPh}_3)][\text{C}_5(\text{CF}_3)_5]$ . Hydrogens and solvent molecules are omitted for clarity. Ellipsoids are depicted with 50% probability level. Color code: grey-carbon; green-fluorine; yellow-bismuth; light-blue-rhodium.

$\text{NPh}_3]$  and  $[\text{Rh}(\text{COD})(\eta^6\text{-BiPh}_3)][\text{C}_5(\text{CF}_3)_5]$  are rare examples of  $\text{NPh}_3$  and  $\text{BiPh}_3$  coordination compounds, respectively.

## Experimental Section

**$[\text{Rh}(\text{COD})(\eta^6\text{-NPh}_3)][\text{C}_5(\text{CF}_3)_5]$ .** In a dried 10 mL Schlenk tube  $[\text{Rh}(\text{COD})(\text{C}_5(\text{CF}_3)_5)]$  (15 mg, 24  $\mu\text{mol}$ , 1.0 equiv.) and  $\text{NPh}_3$  (5.9 mg, 24  $\mu\text{mol}$ , 1.0 equiv.) were dissolved in anhydrous *n*-pentane and stirred at rt for 3 d, after which a light yellow precipitate formed. The residue was decanted and washed with anhydrous *n*-pentane (2×1 mL) and the remaining solvent was removed under high vacuum to afford  $[\text{Rh}(\text{COD})(\eta^6\text{-NPh}_3)][\text{C}_5(\text{CF}_3)_5]$  (21 mg, 24  $\mu\text{mol}$ , quant.) as a yellow solid.

$^1\text{H NMR}$  (401 MHz,  $\text{CD}_2\text{Cl}_2$ )  $\delta$  [ppm] = 7.56–7.51 (m, 4H), 7.41 (tt,  $^3J_{\text{H,H}} = 7.5$  Hz,  $^4J_{\text{H,H}} = 1.2$  Hz, 2H), 7.38–7.34 (m, 4H), 6.35–6.30 (m, 2H), 6.27–6.23 (m, 1H), 5.99–5.95 (m, 2H), 4.59 (s, 4H), 2.47–2.41 (m, 4H), 2.24–2.17 (m, 4H).  $^{13}\text{C}\{^1\text{H}\}$  NMR (151 MHz,  $\text{CD}_2\text{Cl}_2$ )  $\delta$  [ppm] = 142.5 (s, 2 C), 140.4 (s, 1 C), 131.3 (s, 4 C), 128.8 (s, 2 C), 127.5 (s, 4 C), 103.3 (d,  $^1J_{\text{Rh,C}} = 3.3$  Hz, 2 C), 97.5 (d,  $^1J_{\text{Rh,C}} = 2.7$  Hz, 1 C), 88.4 (d,  $^1J_{\text{Rh,C}} = 2.7$  Hz, 2 C), 78.9 (d,  $^1J_{\text{Rh,C}} = 12.5$  Hz, 4 C), 31.9 (s, 4 C).  $^{19}\text{F NMR}$  (377 MHz,  $\text{CD}_2\text{Cl}_2$ )  $\delta$  [ppm] = –50.6 (s, 15F). FT-IR (ATR)  $\nu^-$  [ $\text{cm}^{-1}$ ] = 2890 (w), 2843 (w), 2803 (w), 2285 (w), 1543 (m), 1492 (m), 1347 (m), 1209 (s), 1117 (s), 1005 (w), 879 (w), 800 (m), 757 (m), 703 (s), 632 (s), 511 (m). HRMS (ESI-TOF, negative)  $m/z$  for  $[\text{C}_5(\text{CF}_3)_5]^-$  calculated: 404.9760; measured: 404.9841. EA ( $[\text{Rh}(\text{COD})(\text{NPh}_3)][\text{C}_5(\text{CF}_3)_5]$ ) calculated: C: 50.19% H: 3.16% N: 1.63%; measured: C: 48.69% H: 3.31% N: 1.18%.

**$[\text{Rh}(\text{COD})(\text{PPh}_3)_2][\text{C}_5(\text{CF}_3)_5]$ .** In a dried 10 mL Schlenk tube  $[\text{Rh}(\text{COD})(\text{C}_5(\text{CF}_3)_5)]$  (10 mg, 16  $\mu\text{mol}$ , 1.0 equiv.) and  $\text{PPh}_3$  (8.0 mg, 32  $\mu\text{mol}$ , 2.0 equiv.) were dissolved in anhydrous *n*-pentane and stirred at rt for 3 d, after which an orange precipitate was formed. The residue was decanted and washed with anhydrous *n*-pentane (2×1 mL) and the remaining solvent was removed under high vacuum to afford  $[\text{Rh}(\text{COD})(\text{PPh}_3)_2][\text{C}_5(\text{CF}_3)_5]$  (18 mg, 16  $\mu\text{mol}$ , quant.) as an orange solid.

$^1\text{H NMR}$  (401 MHz,  $\text{CD}_2\text{Cl}_2$ )  $\delta$  [ppm] = 7.46–7.34 (m, 18H), 7.27 (t,  $^3J_{\text{H,H}} = 6.9$  Hz, 12H), 4.54 (s, 4H), 2.51–2.43 (m, 4H), 2.23 (dd,  $^2J_{\text{H,H}} = 16.2$  Hz,  $^3J_{\text{H,H}} = 7.6$  Hz, 4H).  $^{13}\text{C}\{^1\text{H}\}$  NMR (101 MHz,  $\text{CD}_2\text{Cl}_2$ )  $\delta$  [ppm] = 134.0 (t,  $^2J_{\text{P,C}} = 5.8$  Hz, 12 C), 131.1 (s, 6 C), 130.3 (t,  $^1J_{\text{P,C}} = 21.4$  Hz, 6 C), 128.7 (t,  $^3J_{\text{P,C}} = 5.0$  Hz, 12 C), 99.0 (dt,  $^1J_{\text{Rh,C}} = 7.5$  Hz,  $^2J_{\text{P,C}} = 4.6$  Hz, 4 C), 30.6 (s, 4 C).  $^{19}\text{F NMR}$  (377 MHz,  $\text{CD}_2\text{Cl}_2$ )  $\delta$  [ppm] = –50.6 (s, 15F).  $^{31}\text{P}\{^1\text{H}\}$  NMR (162 MHz,  $\text{CD}_2\text{Cl}_2$ )  $\delta$  [ppm] = 26.5 (d,  $^1J_{\text{Rh,P}} = 144.9$  Hz, 2P). FT-IR (ATR)  $\nu^-$  [ $\text{cm}^{-1}$ ] = 3059 (w), 2963 (w), 1533 (m), 1494 (m), 1259 (s), 1211 (s), 1089 (vs), 1014 (vs), 867 (m), 796 (vs), 742 (s), 691 (vs), 632 (s), 533 (s). HRMS (ESI-TOF, positive)  $m/z$  for  $[\text{Rh}(\text{COD})(\text{PPh}_3)_2]^+$  calculated: 735.1817; measured: 735.1849. HRMS (ESI-TOF, positive)  $m/z$  for  $[\text{Rh}(\text{COD})(\text{PPh}_3)]^+$  calculated: 473.0905; measured: 473.1014. HRMS (ESI-TOF, negative)  $m/z$  for  $[\text{C}_5(\text{CF}_3)_5]^-$  calculated: 404.9760; measured: 404.9953. EA ( $[\text{Rh}(\text{COD})(\text{PPh}_3)_2][\text{C}_5(\text{CF}_3)_5]$ ) calculated: C: 58.86%, H: 3.71%; measured: C: 56.91%, H: 3.53%.

**$[\text{Rh}(\text{COD})(\text{AsPh}_3)_2][\text{C}_5(\text{CF}_3)_5]$ .** In a dried 10 mL Schlenk tube  $[\text{Rh}(\text{COD})(\text{C}_5(\text{CF}_3)_5)]$  (15 mg, 24  $\mu\text{mol}$ , 1.0 equiv.) and  $\text{AsPh}_3$  (15 mg, 48  $\mu\text{mol}$ , 2.0 equiv.) were dissolved in anhydrous *n*-pentane and stirred at rt for 16 h, after which an orange precipitate formed. The residue was decanted and washed with anhydrous *n*-pentane (2×1 mL) and the remaining solvent was removed under high vacuum to afford  $[\text{Rh}(\text{COD})(\text{AsPh}_3)_2][\text{C}_5(\text{CF}_3)_5]$  (29 mg, 24  $\mu\text{mol}$ , quant.) as an orange solid.

$^1\text{H NMR}$  (401 MHz,  $\text{CD}_2\text{Cl}_2$ )  $\delta$  [ppm] = 7.41 (t,  $^3J_{\text{H,H}} = 7.1$  Hz, 6H), 7.34–7.31 (m, 12H), 7.27 (t,  $^3J_{\text{H,H}} = 7.6$  Hz, 12H) 4.74 (s, 4H), 2.52–2.43 (m, 4H), 2.22–2.13 (m, 4H).  $^{13}\text{C}\{^1\text{H}\}$  NMR (101 MHz,  $\text{CD}_2\text{Cl}_2$ )  $\delta$  [ppm] =

133.8 (s, 12 C), 132.1 (s, 6 C), 131.2 (s, 6 C), 129.7 (s, 12 C), 94.5 (d,  $^1J_{\text{Rh,C}}=8.9$  Hz, 4 C), 31.3 (s, 4 C).  $^{19}\text{F}$  NMR (377 MHz,  $\text{CD}_2\text{Cl}_2$ )  $\delta$  [ppm] =  $-50.6$  (s, 15F). FT-IR (ATR)  $\nu^-$  [ $\text{cm}^{-1}$ ] = 3058 (w), 2925 (w), 1494 (m), 1437 (m), 1295 (w), 1212 (s), 1116 (s), 999 (m), 867 (w), 801 (w), 734 (m), 690 (m), 633 (m), 482 (m). HRMS (ESI-TOF, positive) m/z for  $[\text{Rh}(\text{COD})(\text{AsPh}_3)]^+$  calculated: 517.0384; measured: 517.0412. HRMS (ESI-TOF, negative) m/z for  $[(\text{C}_5(\text{CF}_3)_5)]^-$  calculated: 404.9760; measured: 404.9775. EA ( $[\text{Rh}(\text{COD})(\text{AsPh}_3)_2][\text{C}_5(\text{CF}_3)_5]$ ) calculated: C: 52.79%, H: 3.45%; measured: C: 53.49%, H: 4.38%.

$[\text{Rh}(\text{COD})(\text{SbPh}_3)_3][\text{C}_5(\text{CF}_3)_5]$ . In a dried 10 mL Schlenk tube  $[\text{Rh}(\text{COD})(\text{C}_5(\text{CF}_3)_5)]$  (15 mg, 24  $\mu\text{mol}$ , 1.0 equiv.) and  $\text{SbPh}_3$  (25 mg, 72  $\mu\text{mol}$ , 3.0 equiv.) were dissolved in anhydrous *n*-pentane and stirred at rt for 3 d, after which an orange precipitate formed. The residue was decanted and washed with anhydrous *n*-pentane (2 $\times$ 1 mL) and the remaining solvent was removed under high vacuum to afford  $[\text{Rh}(\text{COD})(\text{SbPh}_3)_3][\text{C}_5(\text{CF}_3)_5]$  (40 mg, 24  $\mu\text{mol}$ , quant.) as an orange solid.

$^1\text{H}$  NMR (401 MHz,  $\text{CD}_2\text{Cl}_2$ )  $\delta$  [ppm] = 7.43 (tt,  $^3J_{\text{H,H}}=7.4$  Hz,  $^4J_{\text{H,H}}=0.9$  Hz, 9H), 7.26 (t,  $^3J_{\text{H,H}}=7.7$  Hz, 18H), 7.11 (dd,  $^3J_{\text{H,H}}=8.1$  Hz,  $^4J_{\text{H,H}}=1.0$  Hz, 18H), 4.50 (s, 4H), 2.58 (d,  $^2J_{\text{H,H}}=11.1$  Hz, 4H), 2.14 (d,  $^2J_{\text{H,H}}=9.3$  Hz, 4H).  $^{13}\text{C}\{^1\text{H}\}$ NMR (101 MHz,  $\text{CD}_2\text{Cl}_2$ )  $\delta$  [ppm] = 136.0 (s, 18 C), 132.7 (s, 9 C), 131.0 (s, 9 C), 130.0 (s, 18 C), 81.4 (s, 4 C), 32.9 (s, 4 C).  $^{19}\text{F}$  NMR (377 MHz,  $\text{CD}_2\text{Cl}_2$ )  $\delta$  [ppm] =  $-50.7$  (s, 15F). FT-IR (ATR)  $\nu^-$  [ $\text{cm}^{-1}$ ] = 3050 (w), 2919 (w), 1479 (m), 1431 (m), 1213 (s), 1118 (s), 997 (m), 872 (m), 800 (m), 727 (s), 692 (s), 632 (s), 511 (m), 459 (s). HRMS (ESI-TOF, positive) m/z for  $[\text{Rh}(\text{COD})(\text{SbPh}_3)_2]^+$  calculated: 915.0418; measured: 915.0298. HRMS (ESI-TOF, positive) m/z for  $[\text{Rh}(\text{COD})(\text{SbPh}_3)]^+$  calculated: 563.0206; measured: 563.0162. EA ( $\text{C}_{72}\text{H}_{57}\text{F}_{15}\text{RhSb}_3$ ) calculated: C: 51.62%, H: 3.43%; measured: C: 51.78%, H: 3.79%.

$[\text{Rh}(\text{COD})(\eta^6\text{-BiPh}_3)][\text{C}_5(\text{CF}_3)_5]$ . In a dried 10 mL Schlenk tube  $[\text{Rh}(\text{COD})(\text{C}_5(\text{CF}_3)_5)]$  (20 mg, 33  $\mu\text{mol}$ , 1.0 equiv.) and  $\text{BiPh}_3$  (16 mg, 36  $\mu\text{mol}$ , 1.1 equiv.) were dissolved in anhydrous  $\text{CH}_2\text{Cl}_2$  (1 mL) and stirred at rt for 24 h, after which a black precipitate formed. The residue was filtered under inert conditions and the solvent was removed under high vacuum. The residue was washed with anhydrous *n*-pentane (2 $\times$ 1 mL) and the remaining solvent was removed under high vacuum to afford  $[\text{Rh}(\text{COD})(\eta^6\text{-BiPh}_3)][\text{C}_5(\text{CF}_3)_5]$  (27 mg, 26  $\mu\text{mol}$ , 78%) as a yellow solid.

$^1\text{H}$  NMR (401 MHz,  $\text{CD}_2\text{Cl}_2$ )  $\delta$  [ppm] = 7.85 (dd,  $^3J_{\text{H,H}}=8.0$  Hz,  $^4J_{\text{H,H}}=1.3$  Hz, 4H), 7.57 (t,  $^3J_{\text{H,H}}=7.3$  Hz, 4H), 7.45 (tt,  $^3J_{\text{H,H}}=7.4$  Hz,  $^4J_{\text{H,H}}=1.9$  Hz, 2H), 6.97 (tt,  $^3J_{\text{H,H}}=6.3$  Hz,  $^4J_{\text{H,H}}=1.2$  Hz, 1H), 6.64 (dt,  $^3J_{\text{H,H}}=5.6$  Hz,  $^4J_{\text{H,H}}=1.0$  Hz, 2H), 6.37 (t,  $^3J_{\text{H,H}}=6.5$  Hz, 2H), 4.48 (s, 4H), 2.24 (dd,  $^2J_{\text{H,H}}=10.6$  Hz,  $^3J_{\text{H,H}}=4.5$  Hz, 4H), 2.10–2.01 (m, 4H).  $^{13}\text{C}\{^1\text{H}\}$ NMR (151 MHz,  $\text{CD}_2\text{Cl}_2$ )  $\delta$  [ppm] = 137.8 (s, 4 C), 132.0 (s, 4 C), 129.7 (s, 2 C), 125.1 (s, 2 C), 123.3 (s, 1 C), 111.5 (d,  $^1J_{\text{Rh,C}}=3.1$  Hz, 2 C), 106.5 (d,  $^1J_{\text{Rh,C}}=1.9$  Hz, 1 C), 106.0 (d,  $^1J_{\text{Rh,C}}=2.7$  Hz, 2 C), 79.1 (d,  $^1J_{\text{Rh,C}}=12.3$  Hz, 4 C), 31.7 (s, 4 C).  $^{19}\text{F}$  NMR (377 MHz,  $\text{CD}_2\text{Cl}_2$ )  $\delta$  [ppm] =  $-50.5$  (s, 15F). FT-IR (ATR)  $\nu^-$  [ $\text{cm}^{-1}$ ] = 3050 (w), 2962 (w), 2892 (w), 1570 (w), 1493 (s), 1431 (w), 1292 (w), 1206 (s), 1112 (s), 996 (m), 884 (w), 801 (m), 724 (m), 632 (s), 511 (m), 441 (m). HRMS (ESI-TOF, positive) m/z for  $[\text{Rh}(\text{COD})\text{BiPh}_3]^+$  calculated: 651.0971; measured: 651.0917. EA ( $[\text{Rh}(\text{COD})(\text{BiPh}_3)][\text{C}_5(\text{CF}_3)_5]$ ) calculated: C: 40.93% H: 2.58%; measured: C: 41.50%, H: 3.27%.

Deposition numbers CCDC 2329848–2329852 contain the supplementary crystallographic data for this paper. This data is provided free of charge by the joint Cambridge Crystallographic Data Centre and Fachinformationszentrum Karlsruhe Access Structures service [www.ccdc.cam.ac.uk/structures](http://www.ccdc.cam.ac.uk/structures).

The authors have cited additional references within the Supporting Information (Ref. [16–23]).

## Acknowledgements

Gefördert durch die Deutsche Forschungsgemeinschaft (DFG) – Projekt Nummer 387284271 – SFB 1349. The authors acknowledge the assistance of the Core Facility BioSupraMol supported by the DFG. Robin Sievers thanks the Fonds of the Chemical Industry (FCI) for a Kekulé PhD Fellowship. Open Access funding enabled and organized by Projekt DEAL.

## Conflict of Interests

The authors declare no conflict of interest.

## Data Availability Statement

The data that support the findings of this study are available in the supplementary material of this article.

**Keywords:** cyclopentadienyl ligands · fluorinated ligands · rhodium · pnictogens · arene ligands

- [1] a) M. Malischewski, R. Sievers, J. Parche, N. G. Kub, *Synlett* **2023**, 34, 1079–1086; b) O. J. Curnow, R. P. Hughes, *J. Am. Chem. Soc.* **1992**, 114, 5895–5897; c) K. Sünkel, S. Weigand, A. Hoffmann, S. Blomeyer, C. G. Reuter, Y. V. Vishnevskiy, N. W. Mitzel, *J. Am. Chem. Soc.* **2015**, 137, 126–129.
- [2] a) L. V. Dinh, J. A. Gladysz, *Chem. Commun.* **2004**, 998–999; b) L. V. Dinh, J. A. Gladysz, *Chem. Eur. J.* **2005**, 11, 7211–7222.
- [3] a) P. G. Gassman, C. H. Winter, *J. Am. Chem. Soc.* **1986**, 108, 4228–4229; b) M. J. Burk, A. J. Arduengo, III, J. C. Calabrese, R. L. Harlow, *J. Am. Chem. Soc.* **1989**, 111, 8938–8940; c) R. Sievers, M. Reimann, N. G. Kub, S. M. Rupf, M. Kaupp, M. Malischewski, *Chem. Sci.* **2024**. <https://doi.org/10.1039/D3SC06299F>.
- [4] a) D. W. Slocum, T. R. Engelmann, R. L. Fellows, M. Moronski, S. Duraj, *J. Organomet. Chem.* **1984**, 260, C21–C25; b) S. G. Shore, W. L. Hsu, M. R. Churchill, C. Bueno, *J. Am. Chem. Soc.* **1983**, 105, 655–656.
- [5] M. S. Robin Sievers, S. M. Rupf, J. Parche, M. Malischewski, *Angew. Chem. Int. Ed.* **2022**, 61, e202211147.
- [6] J. Parche, S. M. Rupf, R. Sievers, M. Malischewski, *Dalton Trans.* **2023**, 52, 5496–5502.
- [7] a) J. F. Young, J. A. Osborn, F. H. Jardine, G. Wilkinson, *Chem. Commun. (London)* **1965**, 131, <https://doi.org/10.1039/C19650000131>; b) T. M. Trnka, R. H. Grubbs, *Acc. Chem. Res.* **2001**, 34, 18–29; c) H. Guo, Y. C. Fan, Z. Sun, Y. Wu, O. Kwon, *Chem. Rev.* **2018**, 118, 10049–10293; d) J. H. Downing, M. B. Smith, *Comprehensive Coordination Chemistry II*, Vol. 1 (Ed.: J. A. McCleverty, T. J. Meyer), PERGAMON, Oxford, **2003**, pp. 253–296.
- [8] a) N. R. Champness, W. Levason, *Coord. Chem. Rev.* **1994**, 133, 115–217; b) W. Levason, G. Reid, *Coord. Chem. Rev.* **2006**, 250, 2565–2594; c) V. K. Greenacre, W. Levason, G. Reid, *Coord. Chem. Rev.* **2021**, 432, 213698.
- [9] a) E. Becker, C. Slugovc, E. Růba, C. Standfest-Hauser, K. Mereiter, R. Schmid, K. Kirchner, *J. Organomet. Chem.* **2002**, 649, 55–63; b) N. J. Holmes, W. Levason, M. Webster, *J. Organomet. Chem.* **1997**, 545–546, 111–115.
- [10] M. D. Brown, PhD thesis, University of Southampton **2006**.
- [11] L. Zou, S. Guo, H. Lv, F. Chen, L. Wei, Y. Gong, Y. Liu, C. Wei, *Dyes Pigm.* **2022**, 198, 109958.
- [12] D. Hernández-Valdés, G. Meola, H. Braband, B. Spingler, R. Alberto, *Organometallics* **2018**, 37, 2910–2916.
- [13] a) A. J. Carty, N. J. Taylor, A. W. Coleman, M. F. Lappert, *J. Chem. Soc., Chem. Commun.* **1979**, 639–640, <https://doi.org/10.1039/C39790000639>; b) H. Schumann, L. Eguren, *J. Organomet. Chem.* **1991**, 403, 183–193.
- [14] R. D. Chambers, S. J. Mullins, A. J. Roche, J. F. S. Vaughan, *J. Chem. Soc., Chem. Commun.* **1995**, 841–842, <https://doi.org/10.1039/C39950000841>.
- [15] J. Albers, E. Dinjus, S. Pitter, O. Walter, *J. Mol. Catal. A* **2004**, 219, 41–46.

- [16] a) G. R. Fulmer, A. J. M. Miller, N. H. Sherden, H. E. Gottlieb, A. Nudelman, B. M. Stoltz, J. E. Bercaw, K. I. Goldberg, *Organometallics* **2010**, *29*, 2176–2179; b) H. E. Gottlieb, V. Kotlyar, A. Nudelman, *J. Org. Chem.* **1997**, *62*, 7512–7515.
- [17] M. R. Willcott, *J. Am. Chem. Soc.* **2009**, *131*, 13180–13180.
- [18] O. V. Dolomanov, L. J. Bourhis, R. J. Gildea, J. A. K. Howard, H. Puschmann, *J. Appl. Crystallogr.* **2009**, *42*, 339–341.
- [19] G. Sheldrick, *Acta Crystallogr. Sect. A* **2015**, *71*, 3–8.
- [20] a) G. M. Sheldrick, in *Program for Crystal Structure Solution and Refinement*, 2014/7 ed., Göttingen, Germany, **2014**; b) G. Sheldrick, *Acta Crystallogr. Sect. A* **2008**, *64*, 112–122.
- [21] C. F. Macrae, P. R. Edgington, P. McCabe, E. Pidcock, G. P. Shields, R. Taylor, M. Towler, J. van de Streek, *J. Appl. Crystallogr.* **2006**, *39*, 453–457.
- [22] Persistence of Vision Pty. Ltd. Persistence of Vision Raytracer. Ltd., Persistence of Vision Pty. 2004. Retrieved from <http://www.povray.org/download/>.
- [23] S. P. Westrip, *J. Appl. Crystallogr.* **2010**, *43*, 920–925.

---

Manuscript received: January 30, 2024  
Accepted manuscript online: February 21, 2024  
Version of record online: April 11, 2024

---